Monthly Notices of the ROYAL ASTRONOMICAL SOCIETY

MNRAS **523,** L69–L74 (2023) https://doi.org/10.1093/mnrasl/slad060
Advance Access publication 2023 May 25

TRINITY II: The luminosity-dependent bias of the supermassive black hole mass–galaxy mass relation for bright quasars at $z = 6$

Haowen Zhang (张昊文) [1]★ Peter Behroozi [1,2] Marta Volonteri [3] Joseph Silk [3,4,5] Xiaohui Fan [1], James Aird [6,7] Jinyi Yang (杨锦怡) [1]† and Philip F. Hopkins [8]

[1] *Department of Astronomy, University of Arizona, 933 N Cherry Ave., Tucson, AZ 85721, USA*
[2] *Division of Science, National Astronomical Observatory of Japan, 2-21-1 Osawa, Mitaka, Tokyo 181-8588, Japan*
[3] *Institut d'Astrophysique de Paris (UMR 7095: CNRS & Sorbonne Universite), 98 bis Bd. Arago, F-75014 Paris, France*
[4] *Department of Physics and Astronomy, Johns Hopkins University, Baltimore, MD 21218, USA*
[5] *BIPAC, Department of Physics, University of Oxford, Keble Road, Oxford OX1 3RH, UK*
[6] *Institute for Astronomy, University of Edinburgh, Royal Observatory, Edinburgh EH9 3HJ, UK*
[7] *Department of Physics and Astronomy, University of Leicester, University Road, Leicester LE1 7RH, UK*
[8] *Theoretical Astrophysics, California Institute of Technology, Pasadena, CA 91125, USA*

Accepted 2023 May 17. Received 2023 May 16; in original form 2023 March 7

ABSTRACT

Using recent empirical constraints on the dark matter halo–galaxy–supermassive black hole (SMBH) connection from $z = 0$–7, we infer how undermassive, typical, and overmassive SMBHs contribute to the quasar luminosity function (QLF) at $z = 6$. We find that beyond $L_{\rm bol} = 5 \times 10^{46}$ erg s^{-1}, the $z = 6$ QLF is dominated by SMBHs that are at least 0.3 dex above the $z = 6$ median $M_\bullet$–M_* relation. The QLF is dominated by typical SMBHs (i.e. within ±0.3 dex around the $M_\bullet$–M_* relation) at $L_{\rm bol} \lesssim 10^{45}$ erg s^{-1}. At $z \sim 6$, the intrinsic $M_\bullet$–M_* relation for all SMBHs is slightly steeper than the $z = 0$ scaling, with a similar normalization at $M_* \sim 10^{11}$ M$_\odot$. We also predict the $M_\bullet$–M_* relation for $z = 6$ bright quasars selected by different bolometric luminosity thresholds, finding very good agreement with observations. For quasars with $L_{\rm bol} > 3 \times 10^{46}$ (10^{48}) erg s^{-1}, the scaling relation is shifted upwards by ∼0.35 (1.0) dex for 10^{11}M$_\odot$ galaxies. To accurately measure the intrinsic $M_\bullet$–M_* relation, it is essential to include fainter quasars with $L_{\rm bol} \lesssim 10^{45}$ erg s^{-1}. At high redshifts, low-luminosity quasars are thus the best targets for understanding typical formation paths for SMBHs in galaxies.

Key words: galaxies: evolution – galaxies: haloes – quasars: supermassive black holes.

1 INTRODUCTION

The supermassive black hole (SMBH) masses of high-redshift quasars contain critical information on (1) the formation and growth of SMBHs at high redshifts; (2) the feedback from active SMBHs (also called active galactic nuclei, AGN) on their host galaxies in the early Universe, and (3) the build-up of the galaxy–SMBH mass connection. Consequently, there have been many high-redshift quasar surveys aimed at studying their demography. Currently, there are 275 quasars known at $z > 6$ (Fan, Banados & Simcoe 2023). Due to the sheer brightness of high-redshift quasars, it is impractical to measure their host galaxy properties by fitting galaxy spectral energy distributions (SEDs). Therefore, galaxy dynamical masses are often used as a proxy for stellar masses. The measurement of galaxy dynamical mass relies on the high spatial resolution and sensitivity of interferometric radio observations. As a result, the existing galaxy mass measurements have been made predominantly by the Atacama Large Millimeter Array (ALMA; see the compilation by Izumi et al. 2021 and references therein). With the launch of *JWST*, we are finally able to measure host galaxies' stellar masses from rest-frame optical light (e.g. Ding et al. 2022) for at least some high-redshift quasars. At face value, these quasars seem to lie well above the local SMBH mass-galaxy mass ($M_\bullet$–M_*) relation, i.e. having SMBHs that are ∼1 dex more massive than those typical for $z = 0$ galaxies. However, this higher observed $M_\bullet$–M_* relation at $z = 6$ can result from systematic effects. Specifically, the bright quasar sample may be biased towards overmassive SMBHs when there is scatter around the intrinsic $M_\bullet$–M_* scaling relation. These quasars are often selected using flux-limited photometric surveys in the optical and infrared wavebands. When SMBHs have similar Eddington ratios, overmassive objects (compared to the median $M_\bullet$–M_* relation) would be brighter, and will be overrepresented in the selected sample (also known as Lauer bias; Lauer et al. 2007). With a given intrinsic $M_\bullet$–M_* relation and Eddington ratio distribution, the magnitude of Lauer bias increases with the scatter in $M_\bullet$ at fixed M_*, since larger scatter leads to more overmassive SMBHs in the quasar sample. In the absense of scatter around the $M_\bullet$–M_* relation, there will be *no* such selection bias, because every single quasar in the sample will lie perfectly on the scaling relation. To estimate the extent of Lauer bias, one thus needs: (1) the scatter around the intrinsic $M_\bullet$–M_* relation; and (2) the underlying Eddington ratio distributions for SMBHs in different galaxies (see e.g. Li et al. 2022).

★ E-mail: hwzhang0595@arizona.edu
† Strittmatter Fellow.

In this work, we measure the effect of selection bias on the $M_\bullet$–M_* relation for $z \sim 6$ quasars with TRINITY (Zhang et al. 2023). TRINITY is an empirical model of the dark matter halo–galaxy–SMBH connection from $z = 0$–10. With joint constraints from galaxy observations from $z = 0$–10 and SMBH observations from $z = 0$–6.5, TRINITY reconstructs consistent SMBH growth histories and Eddington ratio distributions, both of which are functions of halo/galaxy mass and redshift. This information enables us to create mock luminosity-selected quasar samples and directly compare their $M_\bullet$–M_* relations with the intrinsic relation for *all* $z \sim 6$ SMBHs. This work is timely for the beginning of the *JWST* era, because our results will: (1) predict the offset in the observed $M_\bullet$–M_* relation versus. the intrinsic relation, as a function of quasar luminosity; (2) quantify the extent to which pure selection bias can explain the apparent redshift evolution in the $M_\bullet$–M_* relation from $z = 0$ to $z = 6$; and (3) point future *JWST* observations towards better quasar samples for more accurate measurement of the $M_\bullet$–M_* relation at high redshifts. These predictions are directly testable by future *JWST* observations.

The paper is organized as follows. Section 2 covers methodology. In Section 3, we describe the dark matter simulation and galaxy/SMBH observations used to constrain TRINITY. Section 4 presents our findings on the quasar mass/luminosity bias at $z = 6$. Finally, we present conclusions in Section 5. In this work, we adopt a flat Lambda cold dark matter cosmology with parameters ($\Omega_m = 0.307$, $\Omega_\Lambda = 0.693$, $h = 0.678$, $\sigma_8 = 0.823$, and $n_s = 0.96$) consistent with Planck results (Planck Collaboration 2016). We use data sets that adopt the Chabrier stellar initial mass function (Chabrier 2003), the Bruzual & Charlot (2003) stellar population synthesis model, and the Calzetti dust attenuation law (Calzetti et al. 2000). Halo masses are calculated following the virial overdensity definition from Bryan & Norman (1998).

2 METHODOLOGY

2.1 Why observations alone can constrain the halo–galaxy–SMBH connection

The Sołtan argument (Sołtan 1982) gave rise to the earliest empirical models of SMBH growth: the ratio of the total luminosity output of SMBHs to their $z = 0$ mass density gives the cosmic average radiative efficiency (see e.g. Yu & Tremaine 2002; Marconi et al. 2004). This in turn allows inferring the cosmic average growth history of SMBHs from the redshift evolution of the total luminosity in QLFs.

Recently, studies including Yang et al. (2018) and Aird, Coil & Georgakakis (2018) have measured quasar luminosity distributions as functions of host galaxy mass. At the same time, empirical models of the halo–galaxy connection have succeeded in reconstructing robust galaxy assembly histories that are constrained by galaxy data from $z = 0$–10 (e.g. Behroozi, Wechsler & Conroy 2013; Moster, Naab & White 2013, 2018; Behroozi et al. 2019). These breakthroughs enabled, e.g. Shankar et al. (2020) and Zhang et al. (2023), to apply the Sołtan argument to galaxies split into different stellar mass bins. Specifically, the cumulative SMBH mass growth of a chosen galaxy population is proportional to the net SMBH luminosity of the galaxies' progenitors. This luminosity (of the SMBH progenitors) may be measured by combining measured SMBH luminosities for the correct distribution of galaxy progenitor masses (as a function of redshift), where the galaxy progenitor mass distribution is given by the above-mentioned constraints on galaxy growth histories. The radiative efficiency (which allows inferring the SMBH growth history) is then given by the ratio of the galaxies' net SMBH progenitor luminosity to the galaxies' $z = 0$ SMBH masses. Applying the Sołtan argument in this way yields simultaneous growth histories of galaxies and SMBHs, and in particular constrains the evolution of the SMBH mass – galaxy mass relation with redshift. Based on TRINITY's predicted SMBH growth histories in different halo/galaxy populations, we modelleded their mass and Eddington ratio distributions, which are constrained by SMBH observations, e.g. quasar luminosity distributions as functions of stellar mass, and total quasar luminosity functions (QLFs).

TRINITY also explicitly models the scatter around the median $M_\bullet - M_*$ relation, which is constrained by the shape of active SMBH mass functions. Specifically, a bigger (smaller) scatter around the $M_\bullet - M_*$ relation leads to a stronger (weaker) Eddington bias (Eddington 1913), which would flatten (steepen) the active SMBH mass functions. With inferred SMBH Eddington ratio distributions and the $M_\bullet - M_*$ scatter, TRINITY is well positioned to predict Lauer bias. Constraints on the Lauer bias come from comparing active SMBH mass functions to the expected total SMBH mass function arising from the SMBH–galaxy relationship constrained above, as well as measured Eddington ratios for bright quasars. Stronger Lauer bias results in overmassive black holes being more likely to be active; similarly, stronger Lauer bias also results in lower Eddington ratios at fixed luminosity (as only the most massive black holes are then allowed to be the most luminous). Quantitatively, we find that all active SMBHs with different $M_\bullet$ are accreting at around the Eddington rate at z $\sim$ 6. This is constrained by the facts that: (1) there are very few observed low-mass quasars with super-Eddington accretion at these redshifts (e.g. Shen et al. 2019); (2) lower Eddington ratios and/or broader Eddington ratio distributions will underproduce the active SMBH functions at high redshifts.

Finally, we have verified that TRINITY predictions are robust against changes in model parametrizations and input assumptions. We experimented with many model variants by changing, for example: (1) the way to parametrize the $M_\bullet - M_*$ relation; (2) Eddington ratio distribution shapes; (3) SMBH merger prescriptions; (4) AGN obscuration corrections; (5) AGN bolometric corrections; we found no qualitative change in our predictions, when the input observations were self-consistent with each other. For full details, we refer readers to the Appendices of Zhang et al. (2023).

2.2 Implementation overview

Here, we give a brief overview of TRINITY. For full details, we refer readers to Zhang et al. (2023).

TRINITY parametrizes the halo–galaxy connection similarly to the UNIVERSEMACHINE: the galaxy star formation rate (SFR) is a double-power law of the galaxy's peak halo mass, and the fraction of star-forming galaxies is a sigmoid function of halo mass. Both functions are allowed to evolve with redshift, which are constrained by galaxy data sets. This parametrization has been well-tested in Behroozi et al. (2019), and gives robust inference of the halo–galaxy connection from joint observational galaxy constraints.

We make the galaxy–SMBH connection in TRINITY by parametrizing the $M_\bullet$–$M_{\rm bulge}$ relation as a redshift-dependent power-law. To convert galaxy total masses into bulge masses, we use a redshift-dependent $M_{\rm bulge}$–M_* scaling relation that is fit to Sloan Digital Sky Survey (SDSS) and Cosmic Assembly Near-infrared Deep Extragalactic Legacy Survey (CANDELS) observations (for full details, see Zhang et al. 2023). We calculate average SMBH growth rates in different halo/galaxy populations by tracking the change in typical $M_\bullet$ between successive snapshots. We then convert average SMBH growth rates into AGN Eddington ratio distributions with the following AGN properties chosen from the parameter space:

(1) fractional contributions from SMBH accretion versus SMBH mergers; (2) the AGN energy efficiency; (3) the AGN duty cycle; and (4) Eddington ratio distribution shapes. With SMBH masses and Eddington ratio distributions fully parametrized, we generate SMBH observables including QLFs, quasar luminosity distributions as functions of host galaxy mass, active SMBH mass functions, and the $z = 0$ $M_\bullet$–$M_{\rm bulge}$ relation. In all these calculations, we assume that active SMBHs follow the same $M_\bullet$–$M_{\rm bulge}$ relation as dormant SMBHs. We include systematic and selection effects such as AGN obscuration and bolometric corrections, and finally compare the generated statistics with observed data. In the fiducial TRINITY model, we parametrize the SMBH–galaxy mass connection as a power-law $M_\bullet$–$M_{\rm bulge}$ relation that can evolve with redshift. But we also showed in Appendix E2 of Zhang et al. (2023) that we get consistent $M_\bullet$–M_* relations regardless of whether we parametrize the $M_\bullet$–$M_{\rm bulge}$ relation or the $M_\bullet$–M_* relation directly. Given the growing interest in the $M_\bullet$–M_* relation across cosmic time, we focus our discussion on the bias in the $M_\bullet$–M_*, rather than the $M_\bullet$–$M_{\rm bulge}$ relation in this work.

Using a custom Metropolis Markov Chain Monte Carlo algorithm (based on Haario, Saksman & Tamminen 2001), we create ∼2 million mock universes and compare them with our data compilation. Through such comparisons, we obtain the joint posterior distribution of TRINITY model parameters, and characterize the best-fitting halo–galaxy–SMBH connection, as well as the corresponding uncertainties.

3 SIMULATIONS AND DATA CONSTRAINTS

3.1 Dark matter halo statistics

TRINITY traces statistical halo assembly histories obtained from N-body simulations of dark matter haloes, instead of keeping track of individual haloes/galaxies across cosmic time. Specifically, halo mass functions are obtained from Tinker et al. (2008), with the corrections in Behroozi et al. (2013) to: (1) use halo peak mass instead of current mass; (2) improve the accuracy at higher redshifts; and (3) include satellite haloes. We refer readers to Appendix G of Behroozi et al. (2013) for details. These mass functions are valid for studying halo evolution from at least 10^{10} to 10^{15} $M_\odot$.

Haloes experience mass growth via both accretion and mergers. The average halo accretion histories in this work are described by the fitting formulae in Appendix H of Behroozi et al. (2013). Halo merger rates are fitted from the mock catalogues of the UNIVERSEMACHINE (Behroozi et al. 2019). The fitting formulae for halo mergers are presented in Appendix A of Zhang et al. (2023).

3.2 Observational data constraints

We use the following galaxy data to constrain the halo–galaxy connection: stellar mass functions ($z = 0$–8), galaxy quenched fractions (QFs, $z = 0$–4), average specific SFRs, ($z = 0$–8), cosmic SFRs ($z = 0$–10), and galaxy ultraviolet luminosity functions (UVLFs, $z = 8$–10). We refer readers to section 2.2 and Appendix C of Behroozi et al. (2019) for full details about all adopted galaxy data.

To constrain the galaxy–SMBH connection, we have compiled the following SMBH observables: X-ray QLFs (from Ueda et al. 2014, $z = 0$–5), X-ray quasar probability distribution functions (from Aird et al. 2018, $z = 0.1$–2.5), optically-selected active black hole mass functions (from Schulze & Wisotzki 2010, Schulze et al. 2015, and Kelly & Shen 2013, $z = 0.2$–5), the $z = 0$ $M_\bullet$–$M_{\rm bulge}$ relation (Häring & Rix 2004; Beifiori et al. 2012; Kormendy & Ho 2013; McConnell & Ma 2013; Savorgnan et al. 2016), and the observed $M_\bullet$ distribution of high redshift ($z \sim 6$) bright quasars (Shen et al. 2019). These SMBH data cover $z = 0$–6.5. For more details about these SMBH observables, see section 3.2.2 of Zhang et al. (2023).

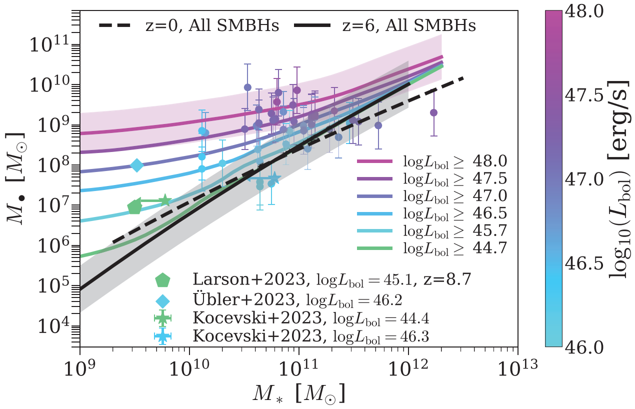

Figure 1. The $z = 6$ median $M_\bullet$–M_* relation for quasars with different bolometric luminosity thresholds. The red shaded region is the 1−σ spread around the median scaling relation for quasars (∼0.6 dex), which includes the random scatter in observed $M_\bullet$ when using virial estimates. This lognormal scatter is nearly luminosity-independent, so we only show it for the brightest quasars for clarity. The black solid line is the $M_\bullet$–M_* relation for all SMBHs at $z = 6$, and the black shaded region is the intrinsic + observed scatter around the intrinsic $M_\bullet$–M_* relation. The green solid line is the $M_\bullet$–M_* relation for AGNs brighter than $\log L_{\rm bol}[{\rm erg\,s^{-1}}] \geq 44.7$, which is the approximate lower limit for *JWST* to measure $M_\bullet$ via broad emission lines. For comparison, we also show the $z = 0$ relation in the black dashed line. Individual data points are $z \gtrsim 6$ quasars compiled by Izumi et al. (2021). We also show two $z > 5$ AGNs from Kocevski et al. (2023) (stars), the $z = 5.55$ AGN from Übler et al. (2023) (the diamond), and the $z = 8.7$ AGN from Larson et al. (2023) (the pentagon). See Section 4.1 for discussion.

4 RESULTS

4.1 Offsets in the $M_\bullet$–M_* relation for bright quasars versus. all SMBHs at $z = 6$

Fig. 1 shows the the median $M_\bullet$–M_* relation for $z = 6$ quasars from TRINITY, as a function of the lower limit in bolometric luminosity. For reference, the bolometric quasar luminosity limit is $\log L_{\rm bol} \gtrsim 45.5$ for Subaru High-z Exploration of Low-Luminosity Quasars (SHELLQs)–Wide program (Runnoe, Brotherton & Shang 2012a, b; Matsuoka et al. 2016), and $\log L_{\rm bol} \gtrsim 46.5$ for Pan-STARRS1 (Chambers et al. 2016) and SDSS (Jiang et al. 2016). According to TRINITY, the Eddington ratio distribution is nearly mass-independent at $z = 6$, so more massive black holes are naturally brighter and more likely to be included in the sample. As a result, SMBHs in bright quasars tend to be overmassive compared to their host galaxies. This systematic offset increases with quasar luminosity, from a ∼0.35 dex offset for $\log L_{\rm bol}[{\rm erg\,s^{-1}}] \geq 46.5$ to a ∼1 dex offset for $\log L_{\rm bol}[{\rm erg\,s^{-1}}] \geq 48$, at host stellar masses of $M_* \sim 10^{11}$ $M_\odot$. The shaded region denotes the 1−σ lognormal spread around the median scaling relation for luminosity limited samples, which is ∼0.6 dex across the mass and luminosity ranges at $z = 6$. This total spread includes: (1) the scatter in intrinsic $M_\bullet$ at fixed M_* for luminosity-limited AGNs, which is inferred by TRINITY (∼0.3 dex); and (2) the scatter in observed $M_\bullet$ around the intrinsic values, which we take as 0.5 dex (e.g. Vestergaard & Peterson 2006; Shen et al. 2023). There is no significant evolution in this total scatter with redshift, down

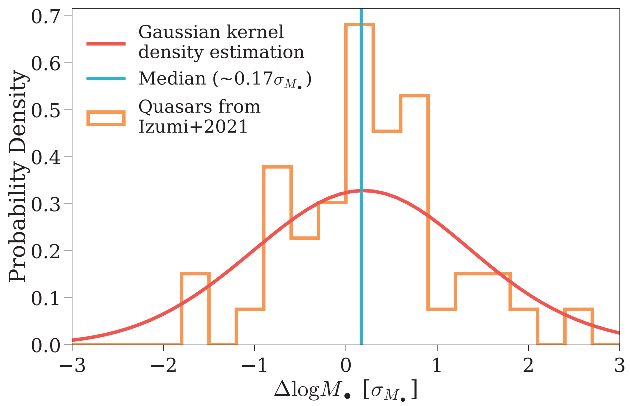

Figure 2. The distribution of Izumi et al. (2021) $z = 6$ quasars' deviation from the TRINITY $M_\bullet$–M_* relations. For each quasar, we calculate the corresponding quasar $M_\bullet$–M_* relation at its bolometric luminosity. The deviation is further normalized by the Gaussian spread, $\sigma_{M_\bullet}$, which is a quadratic sum of the intrinsic scatter around the $M_\bullet$–M_* relation, and the uncertainty in the observed $M_\bullet$. The Gaussian kernel density estimation of the distribution is shown in the red curve. The width of the Gaussian kernel is set to 1 $\sigma_{M_\bullet}$. See Section 4.1.

to $z \sim 0$. Of note, this total scatter is similar to the one around the $M_\bullet$–M_* relation for all SMBHs, which is shown in the black shaded region. This is because both scatters are dominated by the typical scatter in observed $M_\bullet$ around the intrinsic values (0.5 dex). On the other hand, the intrinsic scatter is slightly smaller for the biased sample than for all SMBHs, due to the selection in AGN luminosity. Qualitatively, this trend of increasing $M_\bullet$–M_* normalization with higher luminosity is consistent with the observations, such as the data points compiled by Izumi et al. (2021) (colour-coded by bolometric luminosity). We converted the rest-frame 1450 Å magnitudes from Izumi et al. (2021) into bolometric luminosities using the bolometric correction from Runnoe et al. (2012a, b). We also show the two $z > 5$ low-luminosity AGNs from Kocevski et al. (2023) in star-shape points, as this luminosity-dependent bias in the $M_\bullet$–M_* relation does not change significantly with redshift at $z \gtrsim 6$. The galaxy masses of both AGNs are estimated with SED fitting ignoring potential contributions from their AGNs, and thus should be treated as upper limits. Taken at face value, the $M_\bullet/M_*$ ratios of these two AGNs are qualitatively consistent with TRINITY's predictions. However, further follow-up observations are required for a better measurement of host galaxy masses. We further include in Fig. 1 the $z = 5.55$ AGN from Übler et al. (2023) (the diamond), and the $z = 8.7$ AGN from Larson et al. (2023) (the pentagon). They broadly follow the trend of increasing SMBH mass with increasing bolometric luminosity.

Fig. 2 shows the deviation in $M_\bullet$ from the TRINITY $M_\bullet$–M_* relations for the Izumi et al. (2021) quasar sample. For each observed quasar with a bolometric luminosity L_0, we calculate the TRINITY $M_\bullet$–M_* relation for quasars with $\log L_0 - 0.1\,\mathrm{dex} < L_{\mathrm{bol}} < \log L_0 + 0.1\,\mathrm{dex}$ to ensure a fair comparison. The $M_\bullet$ deviation is divided by the lognormal standard deviation $\sigma_{M_\bullet}$, which is the quadratic sum of the intrinsic TRINITY $M_\bullet$–M_* scatter and the measurement uncertainty in $M_\bullet$ from Izumi et al. (2021). We also show the Gaussian kernel density estimation of the histogram (red solid curve). The kernel width is set to 1 $\sigma_{M_\bullet}$, which is the gaussian scatter of observed $M_\bullet$ deviation given the intrinsic $M_\bullet$–M_* scatter and the typical $M_\bullet$ measurement uncertainty. The distribution of the $M_\bullet$ deviations has a significant amount of scatter around the median value of $\sim 0.17\sigma_{M_\bullet}$, which is $\lesssim 0.1$ dex. Therefore, the apparent evolution in the $M_\bullet$–M_* relation from $z = 0$ to $z = 6$ can be largely explained by Lauer bias.

In the future, more accurate and precise measurements of SMBH and galaxy masses (stellar masses from, e.g. *JWST* and dynamical masses from ALMA) are needed to understand the slight positive deviation as shown in Fig. 2.

According to TRINITY, there is only mild evolution in $M_\bullet$–M_* from $z = 0$ to $z = 6$. This means that typical SMBHs on the intrinsic $M_\bullet$–M_* relation do not experience significant mass build-up before their host galaxies, even though it may be the case for overmassive (and thus brighter) SMBHs in current quasar samples. To understand typical SMBHs and host galaxies' growth histories, it is thus essential to measure the $M_\bullet$–M_* relation of less biased (i.e. fainter) quasar samples. In Fig. 1, we also show the median $M_\bullet$–M_* relation for all SMBHs brighter than $\log L_{\mathrm{bol}}[\mathrm{erg\,s^{-1}}] > 44.7$, which is the lowest AGN luminosity at which *JWST* can still measure $M_\bullet$ reasonably well. At such a low luminosity threshold, the observed $M_\bullet$–M_* relation is very close to the intrinsic relation for all the SMBHs at $\log M_* \gtrsim 10.5$. Therefore, to accurately measure the $z \sim 6$ $M_\bullet$–M_* relation without a severe selection bias, it is essential to focus on fainter quasars at $\log L_{\mathrm{bol}}[\mathrm{erg\,s^{-1}}] \lesssim 45$ in $\log M_* \gtrsim 10.5$ galaxies (e.g. those detected in the SHELLQs, Matsuoka et al. 2022). This is also in line with a series of theoretical studies with Monte Carlo and hydro-dynamical simulations, e.g. Volonteri & Stark (2011), Volonteri & Reines (2016), Marshall et al. (2020), Habouzit et al. (2022). We do caution that for fainter quasars with $\log L_{\mathrm{bol}}[\mathrm{erg\,s^{-1}}] \lesssim 45$, the increasing scatter in the bolometric correction at a fixed UV luminosity for individual objects (see e.g. Runnoe et al. 2012a, b) could add additional uncertainties to bolometric luminosity estimates. This may complicate the interpretation of the $M_\bullet$–M_* relation for fainter quasars in the future.

In addition to the random scatters around intrinsic $M_\bullet$ values, the observed $M_\bullet$ are also subject to potential systematic offsets. Such offsets could be caused by different reasons, e.g. the use of the same virial estimate calibration at both low and high redshifts, which may not be accurate in the real Universe. Qualitatively, if the observed $M_\bullet$ values are systematically overestimated (underestimated), correcting such offsets will lead to better (worse) agreement between TRINITY's predictions and the observations.

In this work, we implicitly assume that all (i.e. whether they are overmassive or not) SMBHs brighter than certain luminosities will be detected in surveys with appropriate flux limits. However, there is another selection bias towards overmassive SMBHs: they are less likely to be outshined by host galaxies. As pointed out by Volonteri, Habouzit & Colpi (2023), only overmassive SMBHs accreting at high Eddington ratios will be detected. Qualitatively, this bias will only increase the offset between the $M_\bullet$–M_* relation for AGNs versus for all SMBHs, and thus does not change our qualitative conclusion. But it takes more detailed modelling of galaxy and SMBH SEDs to quantify this bias, which is beyond the scope of this work. We thus defer the quantification of this bias with TRINITY to future studies.

Finally, we discuss the systematic changes to our result with the intrinsic scatter around the $M_\bullet$–M_* relation. Reines & Volonteri (2015) obtained a $M_\bullet$–M_* relation with much lower normalization than, e.g. Kormendy & Ho (2013) and Greene et al. (2016). This discrepancy could be due to a bigger scatter around the intrinsic $M_\bullet$–M_* relation than commonly estimated. In the current TRINITY model, this scatter is already well constrained to be ~0.3 dex by the shape of active SMBH mass functions, so we opt not to rerun the model by fixing the scatter at a much bigger value, which is not consistent with existing data constraints for TRINITY. Instead, we make the same predictions in Figs. 1 and 2 after increasing the scatter from 0.3 to 0.6 dex, and keeping all the other model parameters unchanged. With a much bigger scatter, more overmassive SMBHs are likely to

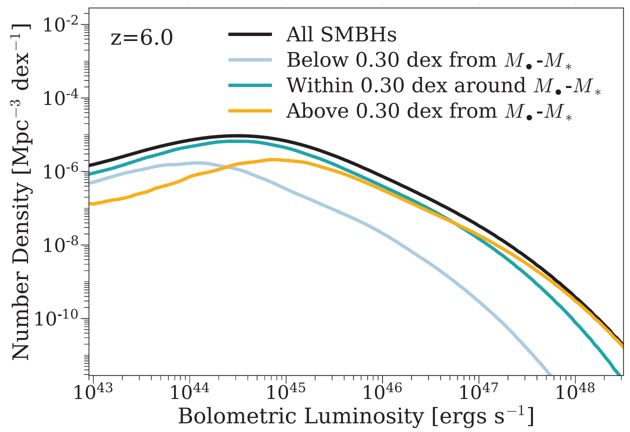

Figure 3. QLFs in bins of the deviation in SMBH mass from the median $M_\bullet$–M_* relation at $z = 6$. See Section 4.2.

exist, and thus the luminosity-dependent bias of the $M_\bullet$–M_* relation becomes even more significant. This effect is the most pronounced with the brightest quasars ($\log L_{\rm bol}[{\rm erg\,s^{-1}}] \geq 48$), which is now ∼2 dex (as opposed to ∼1 dex) overmassive compared to the intrinsic $M_\bullet$–M_* relation. The bigger scatter also leads to the median $M_\bullet$ deviation in Fig. 2 to decrease from $\sim 0.17\sigma_{M_\bullet}$ to $\sim -0.39\sigma_{M_\bullet}$. Such quantitative changes do not change our main conclusions in this work. However, one caveat of this experiment is that this altered model parameter set is not fully consistent with the current data constraints for TRINITY.

4.2 Quasar luminosity functions binned by offset from the $M_\bullet$–M_* relation

Fig. 3 shows QLFs in bins of offset in SMBH mass compared to the median $M_\bullet$–M_* relation at different redshifts. Compared to Fig. 1, Fig. 3 quantifies the Lauer bias in another way, i.e. the amount by which brighter quasars are more likely to be driven by overmassive SMBHs (compared to their host galaxy mass) than typical SMBHs. This effect arises mainly because extremely massive host galaxies are very rare by themselves, and cannot account for the number density of high-mass black holes. According to TRINITY, overmassive SMBHs (>0.3 dex above the median $M_\bullet$–$M_{\rm bulge}$ relation) dominate QLFs at $\log_{10} L_{\rm bol}[{\rm erg\,s^{-1}}] \gtrsim 46.7$ and $z \sim 6$. Typical SMBHs within 0.3 dex around the intrinsic $M_\bullet$–M_* relation dominate the QLF at $\log L_{\rm bol}[{\rm erg\,s^{-1}}] \lesssim 45$. This quantitatively demonstrates the necessity of including fainter AGNs when comparing the $M_\bullet$–M_* relations from the local Universe versus $z \sim 6$ SMBHs.

5 CONCLUSIONS

In this work, we examine the systematic bias in the observed $M_\bullet$–M_* relation for luminosity-limited quasar samples, as well as contributions to the $z = 6$ quasar bolometric luminosity function from SMBHs at different offsets relative to the $z = 6$ $M_\bullet$–M_* relation. Compared to previous studies like Li et al. (2022) that adopt empirically determined Eddington ratio distributions and intrinsic $M_\bullet$–M_* relations at $z = 0$, we make inferences based on the joint SMBH mass–Eddington ratio distributions at different redshifts from TRINITY, which are: (1) explicitly constrained by galaxy and SMBH data (Section 3) and 2) self-consistent with the reconstructed SMBH growth histories. Our key findings are:

(i) At $z \sim 6$, the $M_\bullet$–M_* relation for bright quasars selected by bolometric luminosity ($L_{\rm bol}$) is significantly higher than the intrinsic relation for all SMBHs. This is because there is scatter around the intrinsic $M_\bullet$–M_* relation, and we can only probe the most luminous AGN, which are overmassive compared to the intrinsic $M_\bullet$–M_* relation. With a luminosity threshold of $\log L_{\rm bol}[{\rm erg\,s^{-1}}] > 46.5$ (48), the median $M_\bullet$ is higher by 0.35 (1.0) dex for bright quasars than for typical black holes in $M_* = 10^{11}\,{\rm M_\odot}$ host galaxies. Fainter quasars with $\log L_{\rm bol}[{\rm erg\,s^{-1}}] \lesssim 45$ in $\log M_* \gtrsim 10.5$ galaxies have average $M_\bullet$ very close to the typical $M_\bullet$–M_* relation for all (active and non-active) SMBHs. Although the detected overmassive and bright SMBHs may have grown in mass significantly before their host galaxies, this is not the case for typical SMBHs on the intrinsic $M_\bullet$–M_* relation at $z = 6$, for which we are not yet able to measure $M_\bullet$.(Section 4.1, Figs 1 and 2);

(ii) At $z \sim 6$, our predicted luminosity-dependent $M_\bullet$–M_* relation are consistent with observations compiled by Izumi et al. (2021), which are not in the observational constraints for TRINITY. This further demonstrates the validity of the TRINITY model and its predictions. (Section 4.1, Figs 1 and 2);

(iii) At $z \sim 6$, most observed quasars with $L_{\rm bol} \gtrsim 5 \times 10^{46}\,{\rm erg\,s^{-1}}$ have SMBH masses $\gtrsim$ 0.3 dex higher than the median $M_\bullet$–M_* relation. At brighter luminosities, the QLF is increasingly dominated by SMBHs that are overmassive compared to the median $M_\bullet$–M_* relation. This is because overmassive SMBHs are brighter at similar Eddington ratios. At $\log L_{\rm bol}[{\rm erg\,s^{-1}}] \lesssim 45$, the QLF is dominated by typical SMBHs – i.e. those within 0.3 dex of the $M_\bullet$–M_* relation. (Section 4.2, Fig. 3)

In summary, future observational efforts to measure the intrinsic $z \sim 6$ $M_\bullet$–M_* relation should focus on fainter quasars with $\log L_{\rm bol}[{\rm erg\,s^{-1}}] \lesssim 45$. This motivates future observations with *JWST*, one of the few telescopes that can measure both $M_\bullet$ and M_* for these faint objects. At the same time, observations of faint quasars will directly test theoretical models (including TRINITY) and their predictions for the high-redshift galaxy–SMBH mass connection.

ACKNOWLEDGEMENTS

We thank the anonymous referee for the valuable and constructive feedback. We also thank Gurtina Besla, Haley Bowden, Jane Bright, Katie Chamberlain, Jaclyn Champagne, Arjun Dey, Richard Green, Jenny Greene, Kate Grier, Raphael Hviding, Takuma Izumi, Tod Lauer, Junyao Li, Jianwei Lyu, Joan Najita, George Rieke, Marcia Rieke, John Silverman, Fengwu Sun, Wei-Leong Tee, Feige Wang, Ben Weiner, Christina Williams, and Charity Woodrum for very valuable discussions. This research has made extensive use of the arXiv and NASA's Astrophysics Data System. This research used the Ocelote supercomputer of the University of Arizona. The allocation of computer time from the UA Research Computing High Performance Computing at the University of Arizona is gratefully acknowledged. The Bolshoi-Planck simulation was performed by Anatoly Klypin within the Bolshoi project of the University of California High-Performance AstroComputing Center (UC-HiPACC; PI Joel Primack).

DATA AVAILABILITY

The parallel implementation of TRINITY, the compiled data sets (Section 3.2), and the posterior distribution of model parameters are available online.

REFERENCES

Aird J., Coil A. L., Georgakakis A., 2018, MNRAS, 474, 1225
Behroozi P. S., Wechsler R. H., Conroy C., 2013, ApJ, 770, 57
Behroozi P., Wechsler R. H., Hearin A. P., Conroy C., 2019, MNRAS, 488, 3143
Beifiori A., Courteau S., Corsini E. M., Zhu Y., 2012, MNRAS, 419, 2497
Bruzual G., Charlot S., 2003, MNRAS, 344, 1000
Bryan G. L., Norman M. L., 1998, ApJ, 495, 80
Calzetti D., Armus L., Bohlin R. C., Kinney A. L., Koornneef J., Storchi-Bergmann T., 2000, ApJ, 533, 682
Chabrier G., 2003, PASP, 115, 763
Chambers K. C. et al., 2016, preprint (arXiv:1612.05560)
Ding X. et al., 2022, preprint (arXiv:2211.14329)
Eddington A. S., 1913, MNRAS, 73, 359
Fan X., Banados E., Simcoe R. A., 2023, ARA&A, 000, L1
Greene J. E. et al., 2016, ApJ, 826, L32
Haario H., Saksman E., Tamminen J., 2001, Bernoulli, 7, 223
Habouzit M. et al., 2022, MNRAS, 511, 3751
Häring N., Rix H.-W., 2004, ApJ, 604, L89
Izumi T. et al., 2021, ApJ, 914, 36
Jiang L. et al., 2016, ApJ, 833, 222
Kelly B. C., Shen Y., 2013, ApJ, 764, 45
Kocevski D. D. et al., 2023, preprint (arXiv:2302.00012)
Kormendy J., Ho L. C., 2013, ARA&A, 51, 511
Larson R. L. et al., 2023, preprint (arXiv:2303.08918)
Lauer T. R., Tremaine S., Richstone D., Faber S. M., 2007, ApJ, 670, 249
Li J. et al., 2022, ApJ, 931, L11
Marconi A., Risaliti G., Gilli R., Hunt L. K., Maiolino R., Salvati M., 2004, MNRAS, 351, 169
Marshall M. A., Ni Y., Di Matteo T., Wyithe J. S. B., Wilkins S., Croft R. A. C., Kuusisto J. K., 2020, MNRAS, 499, 3819
Matsuoka Y. et al., 2016, ApJ, 828, 26
Matsuoka Y. et al., 2022, ApJS, 259, 18
McConnell N. J., Ma C.-P., 2013, ApJ, 764, 184
Moster B. P., Naab T., White S. D. M., 2013, MNRAS, 428, 3121
Moster B. P., Naab T., White S. D. M., 2018, MNRAS, 477, 1822
Planck Collaboration, 2016, A&A, 594, A13
Reines A. E., Volonteri M., 2015, ApJ, 813, 82
Runnoe J. C., Brotherton M. S., Shang Z., 2012a, MNRAS, 422, 478
Runnoe J. C., Brotherton M. S., Shang Z., 2012b, MNRAS, 427, 1800
Savorgnan G. A. D., Graham A. W., Marconi A. r., Sani E., 2016, ApJ, 817, 21
Schulze A., Wisotzki L., 2010, A&A, 516, A87
Schulze A. et al., 2015, MNRAS, 447, 2085
Shankar F. et al., 2020, MNRAS, 493, 1500
Shen Y. et al., 2019, ApJ, 873, 35
Shen Y. et al., 2023, preprint (arXiv:2305.01014)
Sołtan A., 1982, MNRAS, 200, 115
Tinker J., Kravtsov A. V., Klypin A., Abazajian K., Warren M., Yepes G., Gottlöber S., Holz D. E., 2008, ApJ, 688, 709
Übler H. et al., 2023, preprint (arXiv:2302.06647)
Ueda Y., Akiyama M., Hasinger G., Miyaji T., Watson M. G., 2014, ApJ, 786, 104
Vestergaard M., Peterson B. M., 2006, ApJ, 641, 689
Volonteri M., Reines A. E., 2016, ApJ, 820, L6
Volonteri M., Stark D. P., 2011, MNRAS, 417, 2085
Volonteri M., Habouzit M., Colpi M., 2023, MNRAS, 521, 241
Yang G. et al., 2018, MNRAS, 475, 1887
Yu Q., Tremaine S., 2002, MNRAS, 335, 965
Zhang H., Behroozi P., Volonteri M., Silk J., Fan X., Hopkins P. F., Yang J., Aird J., 2023, MNRAS, 518, 2123

This paper has been typeset from a TEX/LATEX file prepared by the author.